JOURNAL OF CATALYSIS 32, 237–246 (1974)

Optimum Catalyst Pellet Densities Allowing for Density-Dependent Specific Surface

R. R. HUDGINS,* B. KADLEC,† AND P. L. SILVESTON

Department of Chemical Engineering, University of Waterloo, Waterloo, Ontario, Canada

Received July 3, 1973

Past research has demonstrated that for any specific porous, heterogeneous catalyst there will be an apparent density of the catalyst pellet that will result in a maximum volumetric rate of reaction for a given pellet size. This contribution extends earlier work to cases where the specific surface area is also a function of apparent density. A general model of the change of specific surface area with density is proposed. The model is based upon an empirical representation of pore size and surface area data obtained through heat treating the catalyst and a "squashed sphere" model developed to correlate data obtained through die forming of pellets under pressure.

NOMENCLATURE

$\bar{a}$	Wheeler pore radius $2V_g/S_g$ (cm)
D	Diameter of spherical pellet (cm)
$D_{\text{eff}i}$	Effective diffusivity, species i (cm²/sec)
$\mathfrak{D}_{ij}$	Bulk binary diffusivity of i in j (cm²/sec)
$f(y)$	Potential term of kinetic equation
M_i	Molecular weight of species i (g/gmol)
k_{kin}	True rate constant per unit weight of catalyst (gmol/g-sec)
n	Index in Eq. (11)
$\bar{r}$	Mean pore radius (cm)
r_v	Reaction rate per unit volume of catalyst (gmol/cm³-sec)
S_g	Specific surface (m²/g)
S_{ga}	Specific surface due to macropores (m²/g)
S_{gi}	Specific surface due to micropores (m²/g)
S_{gn}	$n = 0$, 1, 2 constants in Eq. (11) (m²/g)
T	Temperature (°K)
V_g	Pore volume per unit mass of catalyst particles (cm³/g)
y	Mole fraction, gas (—)
α	$1 - (M_i/M_j)^{1/2}$
η	Catalyst effectiveness factor (—)
θ	Porosity (—)
ρ_p	Apparent density of catalyst particle (g/cm³)
ρ_t	True or skeletal density of catalyst particle (g/cm³)

* To whom correspondence should be addressed.

† Department of Inorganic Chemistry, Technical University, Prague, Czechoslovakia (deceased).

INTRODUCTION

The thrust of most catalyst development projects is the formulation of the active catalyst phase as opposed to its physical structure. It is usually assumed that order of magnitude changes in selectivity, yield and rate of reaction are possible through the discovery of a more chemically active catalyst phase. It is now recognized that the physical structure of the catalyst is also important. However, the design of the physical structure is a topic which has not been discussed extensively in the literature.

It has been evident since the classic studies of the late 1930's (see Frank-Kamenetskii (*2*) and Wheeler (*12*)) that the structure of the catalyst can influence significantly both selectivity and rate.

Pelleted catalysts of differing densities are readily prepared by impregnating alumina powder with catalyst or catalyst precursors and compressing the treated powder in a pelleting machine using different die pressures. Rao, Wakao, and Smith (*6*) demonstrated an influence of density on both rate and diffusion for the ortho–para hydrogen conversion at 196°C using NiO impregnated alumina. At about the same time, Van Zoonen and Douwes (*10*) of the Koninklijke/Shell Laboratory in Amsterdam found a similar density effect on rate using Co/Mo on alumina catalyst.

Based on the ortho–para hydrogen conversion data, Cunningham and Smith in a 1963 paper (*1*) demonstrated that the opposing effects of apparent pellet density on surface area available for reaction and on pore diffusion led to an optimum density maximizing the reaction rate per unit volume of a catalytic reactor. Pellet size was found to have a large effect on the optimum density. Optimum densities for the reaction with a NiO on Al_2O_3 catalyst were found for the ortho–para H_2 conversion by Cunningham and Smith. We have calculated optimum apparent pellet densities for a commercial V_2O_5 on kieselguhr catalyst for SO_2 oxidation using this approach in an earlier paper (*3*).

A contribution in the 4th International Congress on Catalysis by Slinko (*7*), also deals with catalyst properties required to maximize the rate per unit volume of a catalyst bed. His paper summarizes a body of research by Boreskov and his school. Slinko found that, at a given catalyst activity, the maximum rate per unit volume occurs when the particle size is sufficiently reduced so that diffusion influences on the rate are negligible. He showed how this size may be calculated.

The study of Cunningham and Smith let the specific surface area remain independent of density. This simplification is limited only to a few special cases. Consequently, it is our purpose in this paper to extend the calculation of optimal apparent density to cases where specific surface area changes. To do this we must consider how the change in apparent pellet density is achieved. We examine compression of powders and heat treatment of the formed pellet in this paper. Heat treatment induces pore size changes which are also considered.

SO_2 Oxidation over a Vanadia Catalyst

The effect of pore structure, particularly surface area, on the maximum reaction may be studied as conveniently with a specific reaction and catalyst system as with an arbitrary reaction such as an irreversible first order reaction. Since the mathematical procedures are not an essential part of our study we have chosen to base our illustration of effects on the oxidation of SO_2 over the Czechoslovakian SVD catalyst. Calculation of an optimal apparent pellet density requires both a kinetic model and a relationship between diffusivity and the pore structure. Both are available for SO_2 oxidation with this catalyst.

The kinetic model developed by Kadlec *et al.* (*4*, *5*) for the SVD catalyst is

$$r_v = k_{\text{kin}} f(y) \eta \rho_p, \tag{1}$$

where r_v is the reaction rate in moles per unit time per unit volume of the catalyst, $f(y)$ is a potential term of the kinetic equation, η is the effectiveness factor and ρ_p is the apparent density of the catalyst pellet. Kadlec *et al.* (*4*, *5*) gave an expression for $f(y)$ and an expression for η in terms of reaction parameters. In accordance with an activated site model for catalytic reaction, k_{kin} is assumed to be directly proportional to the specific surface area of the catalyst.

Effective diffusivity of vanadia catalysts can be described by the relation (*3*),

$$D_{\text{eff}_i} = \frac{\theta^{3/2}}{\dfrac{1 - \alpha y_i}{\mathfrak{D}_{ij}} + \dfrac{1.03 \times 10^4}{\bar{r}(T/M_i)^{1/2}}}, \tag{2}$$

where θ is the open porosity. Equation (2) employed the Bruggeman expression for the ratio of the constriction factor to the tortuosity. In the equation, $\bar{r}$ is the mean pore radius, that is, the first moment of the pore size distribution. It has been shown by Kadlec *et al.* that Eq. (2) closely predicts effective diffusivities calculated from kinetic measurements where θ in this case is the total porosity and $\bar{a} = 2\ V_g/S_g$ is used

in place of the mean pore radius. Equation (2) thus relates effective diffusivity to apparent density noting simply that,

$$\theta = 1 - \rho_p/\rho_t, \tag{3}$$

and that

$$\bar{a} = \frac{2(\rho_t - \rho_p)}{\rho_p \rho_t S_g}. \tag{4}$$

The ratio of the two definitions of pore radius, that is, $\bar{a}/\bar{r}$ for many vanadia catalysts, including SVD, is close to unity.

The optimum in reaction rate per unit bed volume occurs because, in the kinetic expression, Eq. (1), η decreases and k_{kin} either remains constant or decreases as the Thiele modulus ϕ increases. This key modulus may be expressed as:

$$\phi = \frac{D}{2}\left(\frac{k_{\text{kin}}\rho_p}{D_{\text{eff}_{SO_2}}}\right)^{1/2}, \tag{5}$$

for the η used in Eq. (1) (*4*, *5*). In Eq. 5, D is the pellet equivalent spherical diameter and $D_{\text{eff}_{SO_2}}$ depends on ρ_p as Eqs. (2) and (3) show. Also, k_{kin} is proportional to S_g. The net effect is that increasing ρ_p increases the Thiele modulus and η is reduced [according to a formula detailed in Refs. (*4*, *5*)]. We will shortly argue that S_g (and thus k_{kin}) will either remain constant or decrease with an increase in ρ_p. As can be seen in Eq. (1), ρ_p appears explicitly in the expression for volumetric rate. Because of the opposing effects of ρ_p on r_v, an optimum apparent density exists.

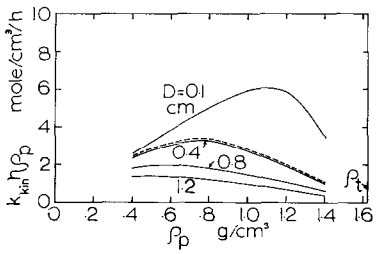

FIG. 1. Effect of apparent density on oxidation rate of SO_2 over SVD vanadia catalyst. Particle diameter of 0.38 cm (– –) is typical of this catalyst in industrial use. Effect of changes in D on optimum are shown. T = 793°K, $\bar{a}/\bar{r}$ = 1.2, ρ_t = 1.62 g/cm³, S_g = 8.4 m²/g.

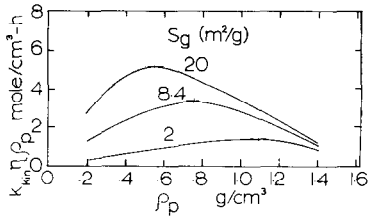

FIG. 2. Effect of apparent density on oxidation rate of SO_2 over SVD vanadia catalyst, showing influence of S_g on optimum. S_g = 8.4 m²/g is the value measured for the industrial catalyst. T = 793°K, $\bar{a}/\bar{r}$ = 1.2, ρ_t = 1.62 g/cm³, D = 0.38 cm.

Assuming, as do Cunningham and Smith (*1*), that the specific surface is independent of apparent density, the optimum ρ_p may be obtained by a one-dimensional search using any one of a number of methods. For illustrative purposes, this was not done, but instead the rate was calculated for various values of ρ_p. Figure 1 shows these values for the SVD catalyst using conditions shown in the caption. The lines show that the optimum density, $(\rho_p)_{\text{opt}}$, is a function of pellet diameter. The optimum is quite pronounced: a 25% shift in density in the optimum region changes the activity by about 10%.

Specific surface area also has an important effect on the optimum. Figure 2 compares the relative rate versus ρ_p behavior for extreme specific surface areas, again assuming the SVD catalyst. Our study of the effect of the pore structure allowing the surface to vary would seem, therefore, to be justified.

The catalyst pore structure normally can be changed only by thermal treatment or by compression if the catalyst is pelleted from a powder. We will consider compression first. The effects of compression will depend on whether the catalyst pore structure is macroporous or microporous or a combination of both.

COMPRESSION-INDUCED CHANGES

a. Macroporous Solids

Catalysts possessing only a macropore structure normally will be agglomerates of

nonporous fine particles or powders. Modeling of particle realignment and slippage which reduce pore volume and surface area per pellet seems beyond reach at present. We have instead chosen to use a model which probably bears little resemblance to the microscopic changes in a pellet during compression, but which adequately represents observed changes resulting from different pelleting pressures. This model, which we refer to as a "squashed sphere" model, provides a means for extrapolation or interpolating data. It may be viewed as an extension of Wheeler's model (*12*) of porous solids composed of rigid spherical granules.

We assume the macroporous solid to be composed of deformable spheres, all having the same diameter. For ease of calculation, we assume further that the balls are in cubic packing and that the point of contact flattens into a square of contact as the lattice is compressed, as shown in Figs. 3 and 4. A square of contact permits calculations to be done by elementary mathematics. The density of the spheres remains uniform so that their volume remains constant.

Compression alters the external surface area which vanishes with the disappearance of the void space between spheres at $\rho_p = \rho_t$. It is evident from Fig. 4 that increasing deformation reduces the void space between the squashed spheres but increases the surface in contact. This surface

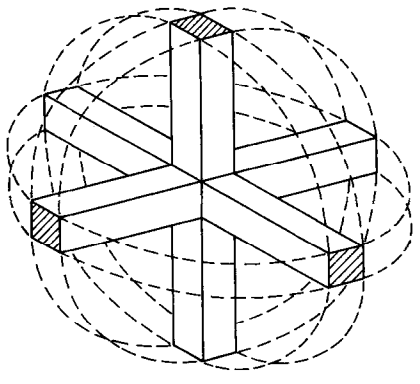

FIG. 3. Schematic showing spherical, disc, and rectangular parallelogram components of a deformable sphere. The hatched areas represent squares of contact with other deformed spheres in the packing.

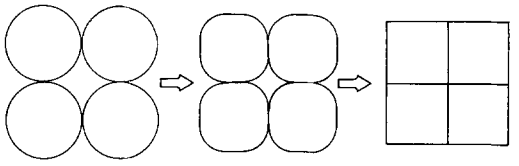

FIG. 4. Two-dimensional representation of squashed sphere model of compression of a granular solid.

is inaccessible so that increasing pressure decreases specific surface.

The results of this model are shown in Fig. 5, in which a normalized form of the specific area is plotted versus the ratio ρ_p/ρ_t. S'_g is defined as:

$$S'_g = \frac{S_g \text{ of squashed sphere}}{S_g \text{ of unsquashed sphere}}.$$

The relationship between S'_g and ρ_p/ρ_t is very close to linear, especially if the region of $\rho_p/\rho_t = 1$ is avoided. This linear relationship would have the form

$$S_g = S_{g_1}(1 - \rho_p/\rho_t), \qquad (6)$$

where S_{g_1} may be considered to be a proportionality constant.

A study of the compression of solids having only macroporosity has not been found. Such a study is available for a solid of mixed microporous and macroporous structures and will be discussed after an analysis of purely microporous solids in compression.

b. Microporous Solids

By definition, microporous solids are ones in which the mean pore diameter is less

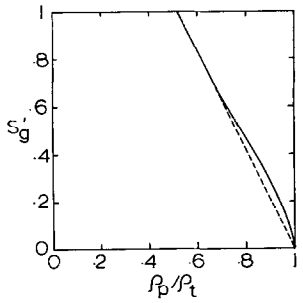

FIG. 5. S'_g vs ρ_p/ρ_t for squashed sphere model (—), showing linear approximation (– –).

than about 200 Å (*8*). Studies of compression of macro–microporous solids (*6*, *10*) show that at the upper limit of compression achievable with hydraulic presses, there is a considerable specific surface still remaining in the solids. It appears, then, that only the macropores are influenced to any extent by compression.

c. *Bidisperse Porous Catalysts*

Bidisperse porous catalysts show two fairly distinct regimes of pores, one micro- and the other macropores. Silica–alumina catalysts (*5*) and other catalysts on alumina supports (*8*) are of this type. The specific surface area will be the sum of the surface areas associated with each pore size range, that is, $S_g = S_{g_a} + S_{g_i}$ where the subscripts a and i denote the macro- and micropore contributions, respectively. We can assume as we did in Sect. (b), that the micropores are unaffected by compression. Compression, however, causes ρ_p to increase towards ρ_t, and invoking our squashed sphere model for the macropores, S_g should decrease approximately linearly as ρ_p decreases. Figure 6 represents assumed behavior of the specific surface with apparent density where the macropores make a significant contribution to the total surface. At point A, the apparent density just suffices for the catalyst pellet to be coherent. Point B in the region $\rho_p/\rho_t \approx 1$ is where all macroporosity would in theory disappear, and, according to the simple idealization, microporosity alone would remain.

Data obtained by Van Zoonen and Douwes (*12*) for a study of compression on pelleted Co/Mo/alumina catalysts is shown

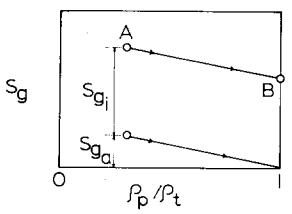

FIG. 6. Schematic interpretation of the effect of compression on the specific surface of a granular solid containing macro- and micro-porosity.

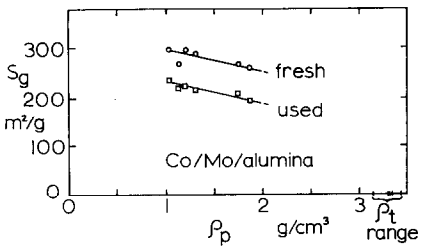

FIG. 7. S_g vs ρ_p for Co/Mo/alumina catalyst. Data of Van Zoonen and Douwes (10).

in Fig. 7. The figure gives S_g vs ρ_p over a twofold change in the apparent density, and indicates a linear relationship between S_g and ρ_p for both fresh and used catalysts. These data are thus consistent with our model and its application to a solid with a bidisperse pore size distribution.

The lines through both sets of data are parallel in Fig. 7 and both sets have identical minimum apparent densities of 1.03 g/cm³. We interpret this to mean that both fresh and used catalyst have the same S_{g_a}. The lower total specific surface for the used catalysts results from a lower S_{g_i}, probably attributable to pore mouth blockage.

Rao, Wakao, and Smith (*6*) in their study of the effect of compression on catalyst performance using a pelleted NiO on alumina catalyst found no change of S_g with pelleting pressure. Their data show that over 96% of the surface area is contributed by the micropores so that the macropore contribution is negligible.

THERMALLY-INDUCED CHANGES

We now turn to heat treatment as a means of raising the apparent pellet density and to the consideration, at least briefly, of the related pore structure changes.

In Fig. 8, we see the results of heat treatment on porous Vycor glass using temperature from 350 and 865°C (*9*). The relationship between S_g and ρ_p is a linear one. This may not be significant of itself since the Vycor sample was held for varying lengths of time at the various temperatures. Hence, a time dependency may have resulted in a fortuitously linear relationship between the points and the value $S_g = 0$ at $\rho_p \approx \rho_t$.

The relationship between the pore radius

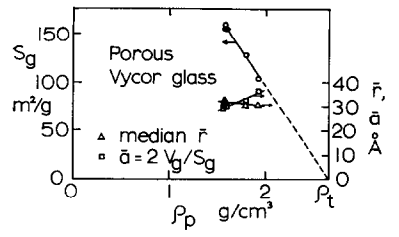

FIG. 8. Specific surface and pore radius as a function of pellet density for porous Vycor glass. Data of Uesugi, Hudgins and Silveston (*9*).

and ρ_p is shown. Values of $\bar{r}$ obtained as medians of the pore size distributions show a slight decrease, although the Wheeler mean radius (8), $\bar{a} = 2\ V_g/S_g$, shows a slight increase with ρ_p. A more pronounced increase in $\bar{r}$ with ρ_p is shown in Fig. 9.

For macroporous solids, it is intuitive and easily demonstrable from our squashed sphere model that $\bar{r}$ or $\bar{a}$ should decrease as ρ_p increase. The squashed sphere model leads to the relationship

$$S_{g\bar{a}} = S_{g\bar{a}}{}^0(1 - \rho_p/\rho_t), \tag{6}$$

where $S_{g\bar{a}}{}^0$ may be considered to be a proportionality constant. From the definitions of V_g and $\bar{a}$, it may be shown that

$$\bar{a} = 2/S_g{}^0\rho_p, \tag{7}$$

consequently $\bar{a}$ should decrease rapidly as ρ_p increases. The thermal treatment results suggest $\bar{a}$ is either roughly independent of ρ_p or increases with ρ_p. Even though S_g decreases with increasing ρ_p, the squashed sphere model cannot be used for thermally induced structure changes.

An explanation for the increase of $\bar{a}$ with

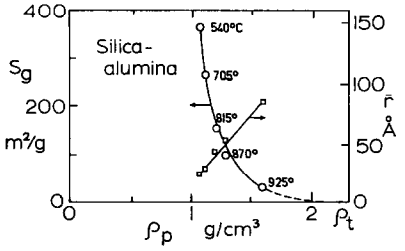

FIG. 9. Specific surface and pore radius as a function of pellet density for silica–alumina catalysts. Data of Weisz and Schwartz (*11*).

ρ_p while S_g decreases is that heat treatment permits the smaller micropores to coalesce into larger ones.

Figure 9 shows another curve of S_g vs ρ_p taken from data of Weisz and Schwartz (*11*) in which silica–alumina catalyst was heat treated for 16 hr at temperatures from 540 to 925°C. In this instance, S_g decreases with increasing ρ_p, but the dependency is not linear.

Figure 9 suggests the following empirical model for thermally induced changes. We note that $dS_g/d\rho_p = 0$ at $\rho_p = \rho_t$, and that $dS_g/d\rho_p$ is negative when $\rho_p < \rho_t$. A simple model satisfying these conditions is:

$$\frac{dS_g}{d\rho_p} = C(\rho_p - \rho_t), \tag{8}$$

where C is a constant. Integration from ρ_p to ρ_t leads to

$$S_g = S_{g_2}(1 - \rho_p/\rho_t)^2. \tag{9}$$

Substitution into the definition of $\bar{a}$

$$\bar{a} = \frac{2}{\rho_p S_{g_2}}\left(\frac{1}{1 - \rho_p/\rho_t}\right). \tag{10}$$

Equations (9) and (10) are in general agreement with the Weisz and Schwartz data, although $\bar{a}$ vs ρ_p does not yield the straight line shown in Fig. 9.

GENERAL MODEL

A general form of Eqs. (6), (7), (9) and (10) is

$$S_g = S_{g_n}(1 - \rho_p/\rho_t)^n, \tag{11}$$

and

$$\bar{a} = \frac{2}{\rho_p S_{g_n}}(1 - \rho_p/\rho_t)^{1-n}, \tag{12}$$

where n can also take on the value zero. In this case S_g is independent of apparent pellet density. This arises for pelleted catalysts when the macropore contribution to S_g is negligible. It may also occur for platelike particles where compression in pelleting might cause platelet alignment simply by reducing the spacing between adjacent platelets without reducing surface area. A summary of the significance of n in this model is given in Table 1.

TABLE 1
MODELS OF SPECIFIC SURFACE DEPENDENCY ON APPARENT DENSITY

	$S_g = S_{gn}(1 - \rho_p/\rho_t)^n$	
n	Model characteristics	Expected physical occurrence
0	S_g remains constant $\bar{a}\downarrow$ as $\rho_p\uparrow$	Macroporous catalysts formed of platelets during compression of pellet
1	"Squashed sphere model" $S_g\downarrow$ and $\bar{a}\downarrow$ as $\rho_p\uparrow$	Macroporous catalysts formed of granular particles during compression of pellet
2	$S_g\downarrow$ and $\bar{a}\uparrow$ as $\rho_p\uparrow$	Microporous catalysts during heat treatment due to coalescence of small pores into larger ones

TABLE 2
PROPERTIES OF SVD CATALYST

ρ_p	particle density or apparent density (g/cm³)	1.170
ρ_t	true density or skeletal density (g/cm³)	1.615
V_g	specific pore volume (cm³/g)	0.236
S_g	specific surface (m²/g)	8.44
$\bar{r}$	median pore radius (Å)	470
$\bar{a}$	Wheeler pore radius (Å)	560

OPTIMAL APPARENT PELLET DENSITY

With the general models for S_g and $\bar{a}$ arising from our squashed sphere model and from a fit of heat treatment data, we can now reexamine the effect of density on rate per unit volume in a catalytic reactor using as our example the oxidation of SO_2 over the SVD catalyst. The properties of the SVD catalyst are given in Table 2. Figures 10 and 11 show the kinetic function curves $k_{kin}\ \eta\rho_p$ vs ρ_p for two different catalyst pellet diameters: 0.38 cm (the measured equivalent spherical diameter) and 0.1, respectively. Conditions of reaction for these calculations are: 793°K, $\bar{a}/\bar{r} = 1.2$, and true (skeletal) density of the catalyst $\rho_t = 1.62$ g/cm³.

Because all of the models were constructed in order that the measured value of S_g (= 8.4 m²/g) would occur at the measured value of ρ_p (= 1.17 g/cm³), the curves in both Figs. 10 and 11 pass through a common point at the apparent density indicated.

A comparison between Figs. 10 and 11 for the effect of diameter shows that the maximum rate increases and occurs at a higher apparent density as the pellet diameter decreases. This behavior has already been rationalized (*3*).

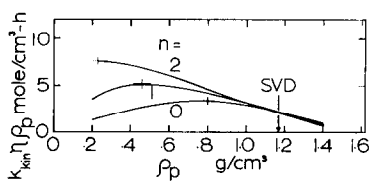

FIG. 10. Effect of apparent density on oxidation rate of SO_2 over SVD vanadia catalyst, showing effect of different assumed dependencies of: $S_g = S_{gn}(1 - \rho_p/\rho_t)^n$; T = 793°K, $\bar{a}/\bar{r} = 1.2$, $\rho_t = 1.62$ g/cm³, $D = 0.38$ cm, $S_g = 8.4$ m²/g at $\rho_p = 1.17$ g/cm³.

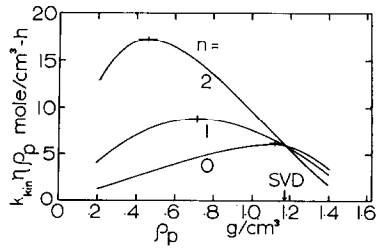

FIG. 11. Effect of apparent density on oxidation rate of SO_2 over SVD vanadia catalyst, showing effect of different assumed dependencies of: $S_g = S_{g0}(1 - \rho_p/\rho_t)^n$; $D = 0.1$ cm and conditions of Fig. 10.

FIG. 12. Photomicrographs of vanadia oxide catalysts for SO_2 oxidation, from scanning electron microscopy. Magnification: 5000×. (a) Cyanamid "Aero" catalyst; (b) Czechoslovakian SVD catalyst.

From either Fig. 10 or 11, it can be seen that the apparent density at which the maximum rate occurs is very sensitive to the dependency of S_g on ρ_p. Also, the maximum reaction rate depends heavily upon the functionality. In Fig. 11, the maximum rates vary almost threefold as the index n of Eq. (11) changes from 0 to 2. There is also a pronounced difference among maximum values for any value of n.

For purposes of making small extrapolations about a given apparent density, it can be seen from Fig. 10 that the change in volumetric rate is relatively insensitive to n for particle diameters practical in fixed beds. Figure 11 shows that the sensitivity n increases at low particle diameters. In both figures the maximum volumetric rate is predicted to be considerably higher than can be achieved at the present apparent catalyst density. The corresponding predicted optimal values of ρ_p are for the most part substantially lower than the measured value. Naturally, there will be practical limits to extrapolation for real catalysts. The region close to ρ_t is of little interest from a physical viewpoint, since it is difficult to bring the pore structure to the point of collapse by either compression or heat treatment of the solid. It is also of little interest from an optimization viewpoint since the specific surface the catalyst tends to zero in on this region.

The range of lower ρ_p values is likewise of no practical interest, since the particle loses mechanical strength in this region, making it unsuitable in a fixed bed.

One may thus conclude that the maximum rate per unit volume for a given catalyst diameter will depend significantly upon the dependency of S_g upon ρ_p. The values of ρ_p at which this maximum occurs is sensitive to such dependency. Thus, the apparent density of the SVD or, indeed any similar catalyst could not be specified to yield a maximum volumetric rate without knowledge of the S_g vs ρ_p relationship.

Topology of SO_2 Oxidation Catalysts

Table 1 suggests certain catalyst characteristics expected to accompany the various dependencies of S_g on ρ_p. Unfortunately, S_g vs ρ_p data are very rare. There is little except intuition to guide in the selection of a model in a given instance.

In order to try to resolve this problem for the SVD catalyst, photomicrographs were prepared of catalyst samples using a scanning electron microscope. For comparison, samples of Cyanamid "Aero" SO_2 oxidation catalyst were also observed. Results are shown in Fig. 12. Figure 12a shows a petal-like or platelet type of structure at a magnification of 5000 times. At the same magnification, SVD catalyst appears in Fig. 12b to be more irregular and crystalline. It would seem from this simple visual description that if these catalysts were subjected to compression, the Cyanamid catalyst would tend to follow Eq. (11) with $n \to 0$, while the SVD catalyst might be described by $0 < n < 1$.

Conclusions

The rate of reaction per unit volume, depends upon the relationship of S_g and ρ_p. The question of optimal catalyst diameter and apparent density cannot be answered without considering the variation of specific surface area with apparent density. There is reasonable although limited evidence for the general models of S_g vs ρ_p and $\bar{a}$ vs ρ_p given by Eqs. (11) and (12), with n varying from 0 to 2 depending on the nature of the catalyst. The question of how to select n in a given instance is likely to remain open for some time because of a lack of experimental information.

Acknowledgments

Much of this manuscript was prepared by one of us (R.R.H.) during a sabbatical leave at the Département de génie chimique, Université de Sherbrooke, Sherbrooke, Québec. The authors acknowledge the help of Mr. M. P. Unni in the performance of several computations. The gift of "Aero" SA catalyst from American Cyanamid Co. is also acknowledged.

References

1. Cunningham, R. E., and Smith, J. M., *AIChE J.* **9**, 419 (1963).
2. Frank-Kamenetskii, D. A., "Diffusion and Heat Exchange in Chemical Kinetics"

(Transl. by N. Thon), Princeton Univ. Press, Princeton, NJ, 1955.

3. KADLEC, B., HUDGINS, R. R., AND SILVESTON, P. L., *Chem. Eng. Sci.* **28,** 935 (1973).
4. KADLEC, B., MICHALEK, J., AND SIMECEK, A., *Chem. Eng. Sci.* **25,** 319 (1970).
5. KADLEC, B., REGNER, A., VOSOLVOBE, J., AND POUR, V., Pap. No. 20, Symp. 3, Novosibirsk, *Int. Congr. Catal., 4th, Moscow, 1968.*
6. RAO, M. R., WAKAO, N., AND SMITH, J. M., *Ind. Eng. Chem. Fundam.* **3,** 127 (1964).
7. SLINKO, M. G., Pap. No. 2, Symp. 3, Novosibirsk, *Int. Congr. Catal., 4th,* Moscow, *1968.*
8. SMITH, J. M., "Chemical Engineering Kinetics." 2nd ed. McGraw-Hill, New York, 1970.
9. UESUGI, S., HUDGINS, R. R., AND SILVESTON, P. L., *J. Amer. Ceram. Soc.* **54,** 199 (1971).
10. VAN ZOONEN, D., AND DOUWES, C. T., *J. Inst. Petrol.* **49,** 383 (1963).
11. WEISZ, P. B., AND SCHWARTZ, A. B., *J. Catal.* **1,** 399 (1962).
12. WHEELER, A., *in* "Catalysis" (P. H. Emmett, Ed.), Vol. 2, Chap. 2. Reinhold, New York, 1955; "Advances in Catalysis" (W. G. Frankenburg, V. I. Komarewsky and E. K. Rideal, Eds.), Vol. 3. Academic Press, New York, 1951.